

The Convergence Indicator: Improved and completely characterized parameter bounds for actual convergence of Particle Swarm Optimization

Bernd Bassimir Alexander Raß* Rolf Wanka
Department of Computer Science
University of Erlangen-Nuremberg, Germany
{bernd.bassimir, alexander.rass, rolf.wanka}@fau.de

Abstract

Particle Swarm Optimization (PSO) is a meta-heuristic for continuous black-box optimization problems. In this paper we focus on the convergence of the particle swarm, i. e., the exploitation phase of the algorithm. We introduce a new convergence indicator that can be used to calculate whether the particles will finally converge to a single point or diverge. Using this convergence indicator we provide the actual bounds completely characterizing parameter regions that lead to a converging swarm. Our bounds extend the parameter regions where convergence is guaranteed compared to bounds induced by converging variance which are usually used in the literature. To evaluate our criterion we describe a numerical approximation using cubic spline interpolation. Finally we provide experiments showing that our concept, formulas and the resulting convergence bounds represent the actual behavior of PSO.

Keywords: Particle swarm optimization · Convergence · Numerical Integration · Heuristics

This research did not receive any specific grant from funding agencies in the public, commercial, or not-for-profit sectors.

1 Introduction

Particle Swarm Optimization (PSO) is a nature-inspired meta-heuristic, first introduced by Eberhart and Kennedy in the year 1995 [KE95], which mimics the behavior of bird flocks and fish swarms. It is designed for so-called continuous black-box optimization problems, i. e., objective functions that are not explicitly provided in a closed formula. The algorithm consists of a set

*Corresponding author

$\{1, \dots, N\}$ of particles, the individuals of the swarm, that move through the D -dimensional continuous search space. Each particle has a position x and a velocity v that are updated via Movement Equations (1) and (2) (see below). Furthermore each particle remembers its best position found so far, its local attractor l , and can access the best position any particle has found, the global attractor g . The swarm operates in discrete time steps, where one iteration consists of one application of the movement equations for each particle.

For each dimension $d \in \{1, \dots, D\}$ particle $n \in \{1, \dots, N\}$ performs its move in iteration $t + 1$ based on the following movement equations:

$$v_{t+1,n,d} = \chi \cdot v_{t,n,d} + c_l \cdot r_{t+1,n,d} \cdot (l_{t,n,d} - x_{t,n,d}) + c_g \cdot s_{t+1,n,d} \cdot (g_{t,n,d} - x_{t,n,d}) \quad (1)$$

$$x_{t+1,n,d} = x_{t,n,d} + v_{t+1,n,d}, \quad (2)$$

where $r_{t+1,n,d}$ and $s_{t+1,n,d}$ are random variables on $[0, 1]$ independently and uniformly drawn in every iteration for every particle and dimension. χ , c_l and c_g are constant parameters chosen by the user. After the particles finish their moves the local and global attractors get possibly updated if better positions were found.

Since its introduction in 1995 PSO has become popular not only among computer scientists as it can be easily implemented and adapted to different problems. Many different variants of PSO were introduced in the literature and analyzed.

A special focus of the analysis of PSO is on the convergence and stagnation, i. e., the premature convergence to non-optimal points, of the swarm. PSO as a meta-heuristic should fulfill the two principals of exploration, i. e., finding new good positions, and exploitation, i. e., improving on already found points. The parameters χ , c_l and c_g have a major impact on the balance between exploration and exploitation. Good choices for the parameters should allow for extensive exploration, while the particles should ultimately converge to the global attractor.

Various publications supply discussions on parameter settings and bounds on them such that convergence can be guaranteed. Some of those which analyze the quality and/or convergence guarantees of different parameter settings theoretically are (among many others) [vdBE02, CE15, Gaz12, HEOB18, JLY07a, JLY07b, Pol09, SW15, Tre03].

In [SW15] Schmitt and Wanka use drift theory to prove the convergence to local optima on one-dimensional objective functions and introduce a slightly modified PSO to extend this analysis to D -dimensional objective functions.

In [vdBE02] Van den Bergh and Engelbrecht introduce a modified PSO algorithm that adds an adaptive noise term at each iteration. They prove that this PSO has a guaranteed convergence.

In [Tre03], Trelea could formulate bounds on the parameters of PSO such that the expected value of the position of a particle converges to the global attractor. The bounds on the parameters presented in [Tre03] are $\chi < 1$, $c_l + c_g > 0$ and $c_l + c_g < 4 \cdot (\chi + 1)$ and these bounds are visualized in Figure 1 if $c_l = c_g = c$ by the triangle enclosed by the black straight line, the right bound of the graph and the χ -axis (i. e., the triangle described by the points $(-1, 0)$, $(1, 4)$, and $(1, 0)$). Please note that there are parameter configurations where the expected values of the particles' positions converge but actually the particles' positions diverge (area between red and black curve in Figure 1 where the black curve is larger than the red curve). On the other hand, there are also cases where the expected values of the particles' positions diverge but actually the particles'

positions converge (area between red and black curve in Figure 1 where the red curve is larger than the black curve). Therefore convergence of the expected value is neither a necessary condition nor a sufficient condition for convergence of the particles' positions. Trelea could identify several different convergence behaviors that the swarm could exhibit based on the parameter selection.

In [JLY07a, JLY07b], Jiang et al. could prove parameter bounds that lead to a convergence of the variance and expected value of the particles' positions given the attractors are constant. Especially if the attractors coincide then the variance converges to zero. If $c_l = c_g = c$ then the area for parameters leading to a convergence of the variance is bounded by the blue curve which represents the inequation $c_l + c_g = 2c \leq 24(1 - \chi^2)/(7 - 5\chi)$ and the χ -axis in Figure 1. In addition to [JLY07a, JLY07b] this bound has been proposed in [Pol09]. Please note that this is a sufficient condition to guarantee convergence of the particles' positions but it is not a necessary condition.

In this paper we focus on the convergence of the swarm, i. e., convergence of the particles' positions, to the global attractor. We mathematically prove and experimentally confirm that there are parameter sets where the expected value and the variance of the particles' positions do not converge, however, the positions of the swarm converge with probability one. Please note that this is not a contradiction, which we will explain in Section 2 after Definition 2 in Example 3 below. In [HEOB18] the quality of different parameter settings is discussed and various parameter sets are experimentally compared. There, good results are also obtained while using parameter sets beyond the bound presented in [JLY07a, JLY07b, Pol09], where the variance of the particles' positions diverges. This indicates that the bound for converging variance is not the actual bound for the convergence of the swarm. If attractors coincide and $c_l = c_g = c$ then the area for parameters leading to a convergence of the particles' positions is bounded by the red curve and the χ -axis in Figure 1. Please note that the slope of the red curve directly to the left of $\chi = 0$ is nearly twice as much as the slope directly to the right of $\chi = 0$, which is not a numerical error. Consequently, it is an interesting observation itself, which could be analyzed more in detail in a future work. We introduce a new measure for the convergence of the particles' positions and provide the actual parameter bounds that lead to the convergence of the particles' positions. These bounds can be obtained with arbitrary precision by numerical approximations using spline interpolation. For $\chi = 0$ this bound can also be obtained by closed theoretical analysis. Hence, we extend the range of parameter settings which provably lead to convergence of PSO as specified in the following theorem.

Theorem 1.

- *The particles' positions converge if the parameters are chosen strictly between the red curve in Figure 1 and the χ -axis.*
- *The particles' positions diverge if the parameters are chosen strictly outside the region between the red curve in Figure 1 and the χ -axis.*

In Section 2 we introduce our new convergence indicator and calculate the difference between two consecutive convergence indicators which can be used to prove bounds on the parameters of the PSO algorithm such that convergence takes place. In Section 3 we explain how these bounds can be calculated numerically and compare the results with experiments confirming the results.

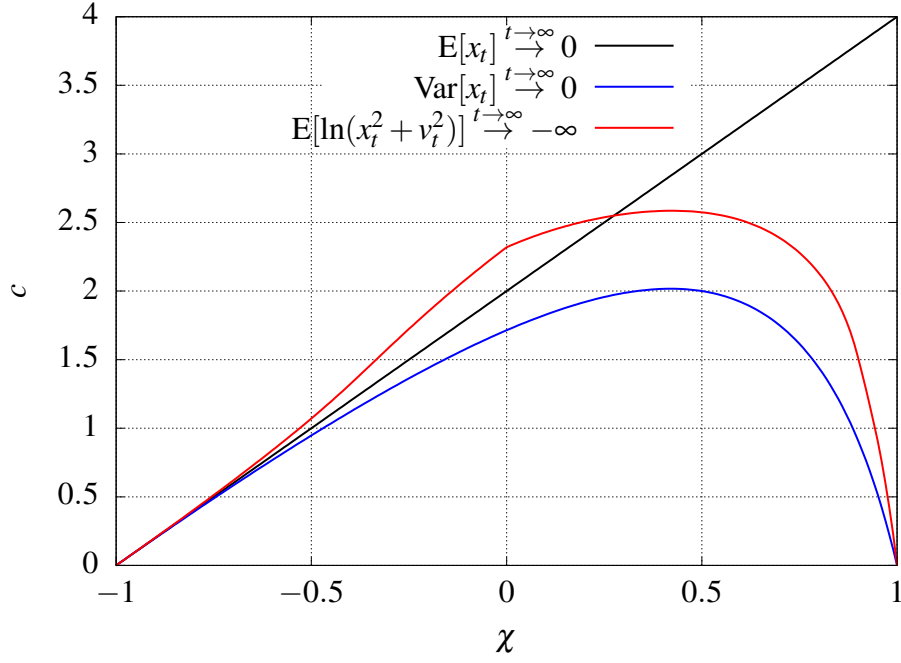


Figure 1: Bounds for the convergence on the expected position to zero (see also [Tre03]), on variance of the position to zero (see also [JLY07a, JLY07b]) and on the expected logarithm of position and velocity to minus infinity

2 Theoretical Analysis on Convergence

First we introduce some simplifications. In practice – at least if in some sense convergence takes place – the positions of the local attractors and the global attractor converge to a single point p in the search space. Then for every $\varepsilon > 0$ there is an iteration t_0 such that the positions of the attractors have Euclidean distance less than ε for all iterations $t > t_0$. If convergence of all positions should take place then the distances of the positions to p have to decrease if they are currently of significantly larger magnitude compared to ε . As this needs to happen for any $\varepsilon > 0$ it is sufficient to check whether positions of the particles converge if attractors exactly have position p . Similar simplifications are commonly used in the literature (see [Tre03]).

Without loss of generality we are assuming that all entries of p are zero and therefore $l_{t,d,n} = g_{t,d,n} = 0$. Then the movement equations are independent for each particle and each dimension. Therefore we omit the indices d for the dimension and n for the particle from now on and analyze only the movement in a single dimension and for a single particle. The movement equations in Equations (1) and (2) degenerate to

$$v_{t+1} = \chi \cdot v_t - c_l \cdot r_{t+1} \cdot x_t - c_g \cdot s_{t+1} \cdot x_t = \chi \cdot v_t - H_{t+1} \cdot x_t \quad (3)$$

$$x_{t+1} = x_t + v_{t+1} = \chi \cdot v_t + (1 - H_{t+1}) \cdot x_t, \quad (4)$$

where r_{t+1} and s_{t+1} are independent and uniformly distributed random variables on $[0, 1]$ and $H_{t+1} \sim c_l \cdot r_{t+1} + c_g \cdot s_{t+1}$. PSO converges to $l_t = g_t = 0$ iff $\lim_{t \rightarrow \infty} x_t = 0$ and $\lim_{t \rightarrow \infty} v_t = 0$. This is equivalent to $\lim_{t \rightarrow \infty} \ln(x_t^2 + v_t^2) = -\infty$.

Therefore, we will use the following definition:

Definition 2 (Convergence Indicator). *We call*

$$\Phi_t := \ln(x_t^2 + v_t^2)$$

the convergence indicator.

With this convergence indicator we can say that PSO converges iff $\lim_{t \rightarrow \infty} \Phi_t = -\infty$. This is the case iff on average the difference $\Phi_{t+1} - \Phi_t$ is negative.

To verify that the expected value and the variance of the position is not a good measure to quantify whether a random variable converges or not we discuss the following example.

Example 3. *Let $(X_t)_{t \geq 0}$ be a random process such that $X_0 = 1$, $\Pr[X_{t+1} = e \cdot X_t] = 1/2$ and $\Pr[X_{t+1} = e^{-2} \cdot X_t] = 1/2$ where e refers to Euler's number (≈ 2.718). Obviously for any $\varepsilon > 0$ we have that $\lim_{t \rightarrow \infty} \Pr[X_t < \varepsilon] = 1$. Nevertheless, $E[X_t] = (e + e^{-2})/2 \cdot E[X_{t-1}] = ((e + e^{-2})/2)^t \xrightarrow{t \rightarrow \infty} \infty$ and $\text{Var}[X_t] \xrightarrow{t \rightarrow \infty} \infty$. In contrast if we analyze $Y_t := \ln(X_t)$ we have $Y_0 = 0$, $\Pr[Y_{t+1} = Y_t + 1] = 1/2$ and $\Pr[Y_{t+1} = Y_t - 2] = 1/2$. Here $E[Y_t] = (1 - 2)/2 + E[Y_{t-1}] = -t/2 \xrightarrow{t \rightarrow \infty} -\infty$ and $E[Y_{t+1} - Y_t] = -1/2 < 0$. The drift of Y_t to $-\infty$ and therefore also the tendency of X_t to zero can easily be noticed in this logarithmic scale.*

Analyzing expected values and variances of positions of particles is also not helpful. Similarly to Example 3 position and velocity of the next iteration can be modeled as (matrix-) multiplication with values of the previous iteration. A better statistic for the analysis is the logarithm of the position. To avoid numerical instabilities we use the square of the position and additionally add the square of the velocity as the velocity also needs to converge to zero.

In the following sections we explain how the expected difference of consecutive convergence indicators can be evaluated as if this difference is negative then convergence can be expected.

2.1 Main case: $c_l \neq 0$ or $c_g \neq 0$

If both parameters c_l and c_g would be zero then PSO performs a deterministic movement independent of the objective function. As this is not profitable we exclude this case for our main analysis and move the respective discussions to Section 2.2.

Similarly as in [OM99] we split the positions of the particles into an angle and a magnitude.

Here we first describe how it is possible to define the current state by the current position and some current angle instead of the current solution. We present an iterative procedure to evaluate the distribution of this angle, which is even independent of the current position. The distribution on this angle enables us to evaluate the expected change in the convergence indicator $E[\Phi_{t+1} - \Phi_t]$.

If no atypical initialization is used then x_t almost surely (in the mathematical sense, see [Dur10]) has a value which is not *exactly* equal to 0, i. e., $\Pr[x_t \neq 0] = 1$. Excluding the event that $x_t = 0$

for any t , we can specify v_t by x_t and an unique additional angle $\alpha_t \in \left(-\frac{\pi}{2}, \frac{\pi}{2}\right)$ such that $v_t = x_t \cdot \tan(\alpha_t)$. Then $v_{t+1} = x_t \cdot (\chi \tan(\alpha_t) - H_{t+1})$ and $x_{t+1} = v_{t+1} + x_t = x_t \cdot (\chi \tan(\alpha_t) + 1 - H_{t+1})$, where $H_{t+1} = c_l r_{t+1} + c_g s_{t+1}$ and s_{t+1}, r_{t+1} are independent and uniformly distributed over $[0, 1]$ as already specified. Therefore

$$\tan(\alpha_{t+1}) = \frac{v_{t+1}}{x_{t+1}} = \frac{\chi \tan(\alpha_t) - H_{t+1}}{\chi \tan(\alpha_t) + 1 - H_{t+1}} = 1 - \frac{1}{1 + \chi \tan(\alpha_t) - H_{t+1}} = f^+(\tan(\alpha_t), H_{t+1}), \quad (5)$$

where

$$f^+(m, h) := 1 - \frac{1}{1 + \chi m - h} \quad (6)$$

This means that the new angle is only dependent on the old angle and the random numbers of the current iteration but it is not dependent on the old position or velocity. χ does not appear as parameter for f^+ as it is a constant.

For any $H_t = c_l \cdot r_t + c_g \cdot s_t$ we can explicitly specify the probability density function. Let $l_H := \min(0, c_l) + \min(0, c_g)$ which is the lower bound on the values which could be observed while evaluating H_t and $u_H := \max(0, c_l) + \max(0, c_g)$ which is the respective upper bound. Furthermore, let $c_{\min} := \min(|c_l|, |c_g|)$ and $c_{\max} := \max(|c_l|, |c_g|)$. Then the probability density function of H_t , where each H_t is the sum of two independent and uniformly distributed random variables, is

$$f_H(h) := \begin{cases} \frac{h-l_H}{|c_l \cdot c_g|} & \text{if } h \in (l_H, l_H + c_{\min}) \\ \frac{1}{c_{\max}} & \text{if } h \in [l_H + c_{\min}, u_H - c_{\min}] \\ \frac{u_H-h}{|c_l \cdot c_g|} & \text{if } h \in (u_H - c_{\min}, u_H) \\ 0 & \text{otherwise.} \end{cases} \quad (7)$$

Please note that this probability density function is also correct if one out of the two values c_l and c_g is zero.

Let $F_{\Delta, t}$ be the cumulative distribution function of α_t . $F_{\Delta, t}$ is a continuous function for any $t > 0$ as

$$\lim_{\delta \rightarrow 0} (F_{\Delta, t+1}(\beta + \delta) - F_{\Delta, t+1}(\beta - \delta)) = \Pr[\alpha_{t+1} = \beta] \quad (8)$$

$$\stackrel{m=\tan(\beta)}{=} \int_{l_H}^{u_H} \Pr[f^+(\tan(\alpha_t), h) = m] f_H(h) dh = 0. \quad (9)$$

This integral has the value zero, because $f^+(m, h)$ is injective in respect to h and therefore the value $\Pr[f^+(\tan(\alpha_t), h) = m]$ can be positive (the value can be at most one) only for a countably finite set of values for h , which has no influence on the value of the integral.

For $t = 0$ the cumulative distribution function $F_{\Delta, t}$ might not be a continuous function as there exists for example the standard idea to use zero as initial value for the velocity resulting in $\alpha_0 = 0$ deterministically. This would result in $F_{\Delta, t}(\beta) = 1$ if $\beta \geq 0$ and $F_{\Delta, t}(\beta) = 0$ otherwise, which is not continuous.

$F_{\Delta, t}$ is by the definition of cumulative distribution functions a monotonic function. In combination with the property that $F_{\Delta, t}$ is continuous (for $t > 0$) we obtain by a theorem of Lebesgue

(a proof can be found, e. g., in [Bot03]) that $F_{\Delta,t}$ is differentiable almost everywhere. We assume to have no pathological example similar to the Cantor (ternary) function [Can84]. Therefore it is assumed that this differentiability almost everywhere can be extended to a derivative of $F_{\Delta,t}$, which will be denoted as $f_{\Delta,t}$. The function $f_{\Delta,t}$ is then the probability density function for α_t and any $t > 0$. In practice (see Section 3) this probability density function exists and it is also a continuous function.

$F_{\Delta,t+1}$ can be calculated using f^+ from Equation (6) and in a second step $F_{\Delta,t}$ by the following formula

$$F_{\Delta,t+1}(\beta) = \Pr[\alpha_{t+1} \leq \beta] \stackrel{m=\tan(\beta)}{=} \int_{l_H}^{u_H} \Pr[f^+(\tan(\alpha_t), h) \leq m] f_H(h) dh, \quad (10)$$

where

$$\Pr[f^+(\tan(\alpha_t), h) \leq m] = \begin{cases} 1 & = 1 & \text{if } \chi = 0 \wedge 1 - \frac{1}{1-h} \leq m \\ 0 & = 0 & \text{if } \chi = 0 \wedge 1 - \frac{1}{1-h} > m \\ \Pr[\alpha_t > \gamma_1] & = 1 - F_{\Delta,t}(\gamma_1) & \text{if } m = 1 \wedge \chi > 0 \\ \Pr[\alpha_t < \gamma_1] & = F_{\Delta,t}(\gamma_1) & \text{if } m = 1 \wedge \chi < 0 \\ \Pr[\alpha_t \notin [\gamma_{\min}, \gamma_{\max}]] & = 1 - F_{\Delta,t}(\gamma_{\max}) + F_{\Delta,t}(\gamma_{\min}) & \text{if } m > 1 \\ \Pr[\alpha_t \in [\gamma_{\min}, \gamma_{\max}]] & = F_{\Delta,t}(\gamma_{\max}) - F_{\Delta,t}(\gamma_{\min}) & \text{if } m < 1 \end{cases} \quad (11)$$

and

$$\gamma_1 = \arctan\left(\frac{h-1}{\chi}\right), \quad \gamma_2 = \arctan\left(\frac{h-1}{\chi} + \frac{1}{\chi \cdot (1-m)}\right), \quad (12)$$

$$\gamma_{\min} = \min(\gamma_1, \gamma_2), \quad \gamma_{\max} = \max(\gamma_1, \gamma_2). \quad (13)$$

This result can be obtained by the following rearrangements (* Please note that for the final simplifications \leq and $<$ are arbitrarily replaced as well as \geq and $>$, because the event that a single value is exactly achieved is either zero in our setting (if $t > 0$) or using a different value has no effect as argued after Equation (9). Also we use that $\gamma_1 \leq \gamma_2 \Leftrightarrow \chi \cdot (1-m) > 0$ in the final step):

$$\Pr[f^+(\tan(\alpha_t), h) \leq m] \quad (14)$$

$$= \Pr\left[1 - \frac{1}{1 + \chi \tan(\alpha_t) - h} \leq m\right] \quad (15)$$

$$= \Pr\left[\begin{array}{l} (\chi = 0 \wedge 1 - \frac{1}{1-h} \leq m) \\ \vee (1 - m = 0 \wedge 0 \leq \frac{1}{1 + \chi \tan(\alpha_t) - h}) \\ \vee \left(1 - m > 0 \wedge 0 \leq \frac{1}{1 + \chi \tan(\alpha_t) - h} \wedge 1 - m \leq \frac{1}{1 + \chi \tan(\alpha_t) - h}\right) \\ \vee \left(1 - m < 0 \wedge \left(0 \leq \frac{1}{1 + \chi \tan(\alpha_t) - h} \vee 1 - m \leq \frac{1}{1 + \chi \tan(\alpha_t) - h}\right)\right) \end{array}\right] \quad (16)$$

$$= \Pr \left[\begin{array}{l} (\chi = 0 \wedge 1 - \frac{1}{1-h} \leq m) \\ \vee (1 - m = 0 \wedge 0 < 1 + \chi \tan(\alpha_t) - h) \\ \vee \left(1 - m > 0 \wedge 0 < 1 + \chi \tan(\alpha_t) - h \wedge 1 - m \leq \frac{1}{1 + \chi \tan(\alpha_t) - h} \right) \\ \vee \left(1 - m < 0 \wedge \left(0 < 1 + \chi \tan(\alpha_t) - h \vee 1 - m \leq \frac{1}{1 + \chi \tan(\alpha_t) - h} \right) \right) \end{array} \right] \quad (17)$$

$$= \Pr \left[\begin{array}{l} (\chi = 0 \wedge 1 - \frac{1}{1-h} \leq m) \\ \vee (1 - m = 0 \wedge \chi > 0 \wedge \alpha_t > \gamma_1) \\ \vee (1 - m = 0 \wedge \chi < 0 \wedge \alpha_t < \gamma_1) \\ \vee (1 - m > 0 \wedge \chi > 0 \wedge \alpha_t > \gamma_1 \wedge \alpha_t \leq \gamma_2) \\ \vee (1 - m > 0 \wedge \chi < 0 \wedge \alpha_t < \gamma_1 \wedge \alpha_t \geq \gamma_2) \\ \vee (1 - m < 0 \wedge \chi > 0 \wedge (\alpha_t > \gamma_1 \vee \alpha_t \leq \gamma_2)) \\ \vee (1 - m < 0 \wedge \chi < 0 \wedge (\alpha_t < \gamma_1 \vee \alpha_t \geq \gamma_2)) \end{array} \right] \quad (18)$$

$$\stackrel{*}{=} \Pr \left[\begin{array}{l} (\chi = 0 \wedge 1 - \frac{1}{1-h} \leq m) \\ \vee (1 - m = 0 \wedge \chi > 0 \wedge \alpha_t > \gamma_1) \\ \vee (1 - m = 0 \wedge \chi < 0 \wedge \alpha_t < \gamma_1) \\ \vee (1 - m > 0 \wedge \gamma_{\min} < \alpha_t < \gamma_{\max}) \\ \vee (1 - m < 0 \wedge (\alpha_t < \gamma_{\min} \vee \gamma_{\max} < \alpha_t)) \end{array} \right] \quad (19)$$

Finally, we return to our initial aim to determine whether the convergence indicator converges to $-\infty$. The differences of subsequent convergence indicators are only dependent on the current angle, which we can see in the following series of equations

$$\mathbb{E}[\Phi_{t+1} - \Phi_t] = \mathbb{E} \left[\ln(x_{t+1}^2 + v_{t+1}^2) - \ln(x_t^2 + v_t^2) \right] = \mathbb{E} \left[\ln \left(\frac{x_{t+1}^2 + v_{t+1}^2}{x_t^2 + v_t^2} \right) \right] \quad (20)$$

$$= \mathbb{E} \left[\ln \left(\frac{(\chi \tan(\alpha_t) - H_{t+1})^2 + (\chi \tan(\alpha_t) - H_{t+1} + 1)^2}{1 + \tan(\alpha_t)^2} \right) \right] \quad (21)$$

$$= \int_{-\frac{\pi}{2}}^{\frac{\pi}{2}} \mathbb{E} \left[\ln \left(\frac{(\chi \tan(\alpha) - H_{t+1})^2 + (\chi \tan(\alpha) - H_{t+1} + 1)^2}{1 + \tan(\alpha)^2} \right) \right] f_{\Delta,t}(\alpha) d\alpha, \quad (22)$$

where $f_{\Delta,t}$ is the probability density function for α_t .

With the helping functions

$$g(\alpha, h) := \ln \left(\frac{(\chi \tan(\alpha) - h)^2 + (\chi \tan(\alpha) - h + 1)^2}{1 + \tan(\alpha)^2} \right) \quad f^{in}(\alpha) = \int_{l_H}^{u_H} g(\alpha, h) \cdot f_H(h) dh \quad (23)$$

we can shorten Equation (22). If we additionally replace the expected value by the respective integral we obtain

$$(22) = \int_{-\frac{\pi}{2}}^{\frac{\pi}{2}} \left(\int_{l_H}^{u_H} g(\alpha, h) \cdot f_H(h) dh \right) f_{\Delta,t}(\alpha) d\alpha = \int_{-\frac{\pi}{2}}^{\frac{\pi}{2}} f^{in}(\alpha) \cdot f_{\Delta,t}(\alpha) d\alpha. \quad (24)$$

In this final equation only $f_{\Delta,t}$ is changing for varying values of t . The corresponding cumulative distribution function $F_{\Delta,t}$ on the angles α_t converge to a unique stationary cumulative distribution function $F_{\Delta,\infty}$. The reason for this cumulative distribution function to be unique is that for

the underlying process and for any starting angle β the set of reachable angles $A_{\alpha_0=\beta,t} := \{\alpha \in (-\pi/2, \pi/2) \mid \forall \varepsilon > 0 : \Pr[\alpha_t \in (\alpha - \varepsilon, \alpha + \varepsilon) \mid \alpha_0 = \beta] > 0\}$ converges to exactly the same set if t tends to infinity. If, e. g., $(0 < \chi < 1 \wedge \max(c_l, c_g) > 1)$, which is true for many common parameter sets, this limit set contains all possible angles in $(-\pi/2, \pi/2)$ as already $A_{\alpha_0=\beta,6} = (-\pi/2, \pi/2)$ for any $\beta \in (-\pi/2, \pi/2)$. In three steps one can move from any starting angle to any open set containing angle zero with positive probability. In three further steps one can move with positive probability from there to any other open set of angles. To make this visible we define the function

$$f^-(m, h) := \frac{1}{\chi \cdot (1 - m)} + \frac{h - 1}{\chi} .$$

This function is the inverse function of f^+ in respect to m , i. e., $f^-(f^+(m, h), h) = m$ and also $f^-(\tan(\alpha_{t+1}), H_{t+1}) = \tan(\alpha_t)$. Then we can observe that the preimage of the angle zero is at least the set $[0, \pi/4]$ as $[0, 1] \subset f^-([0, 0] \times (l_H, u_H))$ and $\arctan(1) = \pi/4$, the preimage of the angles in $[0, \pi/4]$ is at least the set $[0, \pi/2)$ as $[0, +\infty) \subset f^-([0, 1] \times (l_H, u_H))$ and the preimage of the angles $[0, \pi/2)$ is the set of all possible angles in $(-\pi/2, \pi/2)$ as $\mathbb{R} = f^-([0, +\infty) \times (l_H, u_H))$. As H_t has a probability density function which is positive in the interval (l_H, u_H) , this justifies the claim that one can reach any open set containing the angle zero with positive probability within exactly three steps. Additionally, from angle zero one can reach at least the angles in $(-\pi/2, 0)$ as $(-\infty, 0) \subset f^+([0, 0] \times (l_H, u_H))$, from the angles $(-\pi/2, 0)$ one can reach at least the angles in $((-\pi/2, 0) \cup (\pi/4, \pi/2))$ as $((-\infty, 0) \cup (1, +\infty)) \subset f^+((-\infty, 0) \times (l_H, u_H))$ and from the angles in $((-\pi/2, 0) \cup (\pi/4, \pi/2))$ one can reach all possible angles except exactly $\pi/4 = \arctan(1)$ as $(\mathbb{R} \setminus \{1\}) = f^+(((-\infty, 0) \cup (1, +\infty)) \times (l_H, u_H))$. This justifies that one can reach any open set of angles from any open set containing angle zero with positive probability within exactly three steps.

Using the associated stationary probability density function $f_{\Delta, \infty}$ in Equation (24) answers the question whether the particles converge.

Theorem 4. *Let ω be the respective result of Equation (24) using $f_{\Delta, \infty}$ as density function:*

$$\omega = \int_{-\pi/2}^{\pi/2} f^{\text{in}}(\alpha) \cdot f_{\Delta, \infty}(\alpha) d\alpha .$$

- *If $\omega < 0$ then the particles position and velocity converge to the constant attractors.*
- *If $\omega > 0$ then the particles position and velocity do not converge to the constant attractors.*

Proof. For any $\varepsilon > 0$ there exists an iteration t_0 such that $|E[\Phi_{t+1} - \Phi_t] - \omega| < \varepsilon$ for all $t \geq t_0$ which implies that $E[\Phi_t] = E[\Phi_0] + \sum_{i=0}^{t-1} E[\Phi_{i+1} - \Phi_i] \sim \omega \cdot t$. Furthermore, the distribution of $(\Phi_t - E[\Phi_t]) / \sqrt{\text{Var}[\Phi_t]}$ converges to a Gaussian/normal distribution as it can be written as sum of consecutive convergence indicators and the covariance between $E[\Phi_{t_1+1} - \Phi_{t_1}]$ and $E[\Phi_{t_2+1} - \Phi_{t_2}]$ tends to zero if $|t_2 - t_1|$ tends to ∞ (similar arguments apply as for the reasoning on a unique limit distribution on α_t). The vanishing covariance also implies that the variance of Φ_t grows only linearly. Therefore $E[\Phi_t] / \sqrt{\text{Var}[\Phi_t]}$ grows or decreases in the order of \sqrt{t} if $\omega > 0$ or $\omega < 0$ respectively.

These properties imply that if ω is negative then the probability $\lim_{t \rightarrow \infty} \Pr[\Phi_t > \delta] = 0$ for any value $\delta \in \mathbb{R}$. Consequently the position and the velocity needs to converge to zero.

Analogously, if ω is positive the particles positions and velocities will finally diverge. \square

If the result ω evaluates to zero exactly then it has to be decided by different means whether the particles do converge, do not converge or stay in some range as also the initialization can have an effect on this question in this case. Parameters, where the result is exactly zero, are not recommended as also in cases where convergence still appears, the time until sufficient optimization is accomplished would be quite large as the drift of Φ_t to $-\infty$ is very slow and therefore also the convergence of the position to the surroundings of the attractors.

Please note that by Theorem 4 also Theorem 1 is proven as ω is strictly less than zero strictly between the red curve and the χ -axis and ω is strictly greater than zero strictly outside that region.

Theoretically at least the inner integral of Equation (24) can be solved analytically but already displaying the respective solution, which can be obtained by maple or other computer algebra systems, would require more than a page full of formulas. The question how this formula can be evaluated in practice is answered in Section 3.

2.2 Special Case: $c_l = c_g = 0$

In this atypical case where $c_l = c_g = 0$ the velocity deterministically evaluates to $v_t = v_0 \cdot \chi^t$ and therefore

$$x_t = x_0 + \sum_{i=1}^t v_i = x_0 + v_0 \cdot \chi \sum_{i=0}^{t-1} \chi^i = \begin{cases} x_0 + v_0 \cdot \chi \cdot \frac{1-\chi^t}{1-\chi} & \text{if } \chi \neq 1 \\ x_0 + v_0 \cdot t & \text{otherwise.} \end{cases}$$

Consequently, the position converges to some point iff $\lim_{t \rightarrow \infty} \chi^t = 0 \Leftrightarrow |\chi| < 1$. Whether this point is equal to the local and global attractor or even a local or global optimum depends only on the initial choice of x_0 and v_0 and the objective function, but for most settings the answer will very likely be “no”.

For all other sections we assume that either c_l or c_g is not equal to zero.

2.3 Special case: $\chi = 0$

Usually the expected differences of consecutive convergence indicators can not be presented as closed expressions. For $\chi = 0$ there is an exception and we can deduce the closed formula by an approach different from the previous sections. First we describe the positions and velocities of iteration t and $t + 1$ by the position x_{t-1} .

$$\begin{aligned} v_t &= -H_t \cdot x_{t-1}, & x_t &= (1 - H_t) \cdot x_{t-1}, \\ v_{t+1} &= -(1 - H_t) \cdot H_{t+1} \cdot x_{t-1}, & x_{t+1} &= (1 - H_t) \cdot (1 - H_{t+1}) \cdot x_{t-1}, \end{aligned}$$

This can be used to obtain the predicted closed formula in the case where $c_l \neq 0 \neq c_g$:

$$\mathbb{E}[\Phi_{t+1} - \Phi_t] = \mathbb{E}[\ln(x_{t+1}^2 + v_{t+1}^2) - \ln(x_t^2 + v_t^2)] \quad (25)$$

$$= \mathbb{E} \left[\ln \left(\frac{x_{t-1}^2 \cdot (1-H_t)^2 \cdot (H_{t+1}^2 + (1-H_{t+1})^2)}{x_{t-1}^2 \cdot ((1-H_t)^2 + (H_t)^2)} \right) \right] \quad (26)$$

$$= \mathbb{E} \left[\ln \left((1-H_t)^2 \right) + \ln \left(H_{t+1}^2 + (1-H_{t+1})^2 \right) - \ln \left((1-H_t)^2 + (H_t)^2 \right) \right] \quad (27)$$

$$\stackrel{H_t \sim H_{t+1}}{=} \mathbb{E} \left[\ln \left((1-H_t)^2 \right) \right] = \mathbb{E} \left[\ln \left((1-c_l r_t - c_g s_t)^2 \right) \right] \quad (28)$$

$$= \int_0^1 \int_0^1 \ln((1-c_l r - c_g s)^2) dr ds \quad (29)$$

$$= \int_0^1 \left[\frac{1-c_l r - c_g s}{-c_l} \ln((1-c_l r - c_g s)^2) - 2r \right]_0^1 ds \quad (30)$$

$$= \frac{1}{c_l} \int_0^1 \left[-(1-c_l - c_g s) \ln((1-c_l - c_g s)^2) - 2c_l + (1-c_g s) \ln((1-c_g s)^2) \right] ds \quad (31)$$

$$= \frac{1}{c_l} \left[-\frac{(1-c_l - c_g s)^2}{-2c_g} (\ln((1-c_l - c_g s)^2) - 1) \right. \quad (32)$$

$$\left. - 2c_l s + \frac{(1-c_g s)^2}{-2c_g} (\ln((1-c_g s)^2) - 1) \right] \Big|_0^1 \quad (33)$$

$$= \frac{1}{2c_l c_g} \left[(1-c_l - c_g)^2 (\ln((1-c_l - c_g)^2) - 1) - 4c_l c_g - (1-c_g)^2 (\ln((1-c_g)^2) - 1) \right. \quad (34)$$

$$\left. - (1-c_l)^2 (\ln((1-c_l)^2) - 1) - 1 \right] \quad (35)$$

and if $c = c_l = c_g$ then this equation simplifies to

$$\frac{1}{2c^2} \left[(1-2c)^2 \ln((1-2c)^2) - 2(1-c)^2 \ln((1-c)^2) \right] - 3 \quad (36)$$

For $c = c_l = c_g$ this expression is negative iff $c \in (0, \lambda)$ where $\lambda \approx 2.3195565$.

If additionally to $\chi = 0$ also one out of the two values c_l and c_g is zero we obtain a slightly different result. If $c_l = 0, c_g = c$ or $c_l = c, c_g = 0$ we can start with Expression (28) to obtain

$$(28) = \int_0^1 \ln \left((1-c \cdot r)^2 \right) dr = \left[\frac{1-c \cdot r}{-c} \ln \left((1-c \cdot r)^2 \right) - 2r \right] \Big|_0^1 \quad (37)$$

$$= -\frac{1-c}{c} \ln \left((1-c)^2 \right) - 1 \quad (38)$$

This result can also be obtained if one calculates the limit of the result in Equation (35) if c_l or c_g tends to zero.

3 Numeric Identification of Convergence

In this section we explain how the expected difference of consecutive convergence indicators can be evaluated in practice and we present results on evaluations. Finally we compare the obtained results with results from experiments.

A promising approach to solve this problem is cubic spline interpolation [HM76]. By cubic spline interpolation a function which is available at some reference points/knots is interpolated with piecewise cubic polynomials.

3.1 Calculate the cumulative distribution function

We use spline interpolation to calculate the cumulative distribution function $F_{\Delta,t}$ for the angle α_t . As we are mainly interested in the unique limit distribution $F_{\Delta,\infty}$ the start distribution is not important. We use the uniform distribution on the angles in the range $[-\pi/2, \pi/2]$ as starting distribution $F_{\Delta,0}(\beta) = (\beta + \pi/2)/\pi$. To calculate the next cumulative distribution function $F_{\Delta,t+1}$ by $F_{\Delta,t}$ we evaluate $F_{\Delta,t+1}$ at some set of reference knots $\{\beta_1, \beta_2, \dots, \beta_N\}$ by Equation (10), where $\beta_1 = -\pi/2, \beta_N = \pi/2$ and for all i we have $\beta_i < \beta_{i+1}$. To achieve this we evaluate for fixed β_i the integral in Equation (10) again by spline interpolation with a set of reference knots $\{h_1, h_2, \dots, h_M\}$, where $h_1 = l_H, h_M = u_H$ and for all j we have $h_j < h_{j+1}$. For each h_j and fixed β_i the expression $\Pr[f^+(\tan(\alpha_t), h_j) \leq \tan(\beta_i)] \cdot f_H(h_j)$ can be evaluated directly by Equation (7) in combination with Equation (11) as $F_{\Delta,t}$ is already available - at least as an approximation. The respective integral of this expression can then easily be evaluated through the integral on the respective spline interpolation. Finally, we have the pairs $(\beta_i, F_{\Delta,t+1}(\beta_i))$ and therefore we can use them to calculate the next cumulative distribution function $F_{\Delta,t+1}$ as spline interpolation. By this procedure we can iteratively calculate spline interpolations on the cumulative distribution function.

We can stop doing further iterations if the difference of two consecutive cumulative distribution functions is negligible as then the result is close to the unique limit distribution and this distribution can then be used as approximation on $F_{\Delta,\infty}$ and all $F_{\Delta,t}$ for larger values of t .

3.2 Calculate the expected difference of two consecutive convergence indicators

For the evaluation of Equation (24) we use again spline interpolation twice. For the inner integral $f^{in}(\alpha) = \int_{l_H}^{u_H} g(\alpha, h) \cdot f_H(h) dh$ one can evaluate $g(\alpha, h) \cdot f_H(h)$ exactly and we approximate this product by a spline through reference knots $\{h_1, h_2, \dots, h_M\}$, where $h_1 = l_H, h_M = u_H$ and for all j we have $h_j < h_{j+1}$. The integral on this spline can then easily be calculated.

By this helping procedure and the probability density function $f_{\Delta,t}$ at iteration t , which can be obtained as described in the previous section, we can also evaluate the complete integral displayed in Equation 24. For this purpose we evaluate $f^{in}(\alpha) \cdot f_{\Delta,t}(\alpha)$ for reference knots $\{\beta_1, \beta_2, \dots, \beta_N\}$, where $\beta_1 = -\pi/2, \beta_N = \pi/2$ and for all i we have $\beta_i < \beta_{i+1}$. The final result is then obtained by the evaluation of the integral on the corresponding spline.

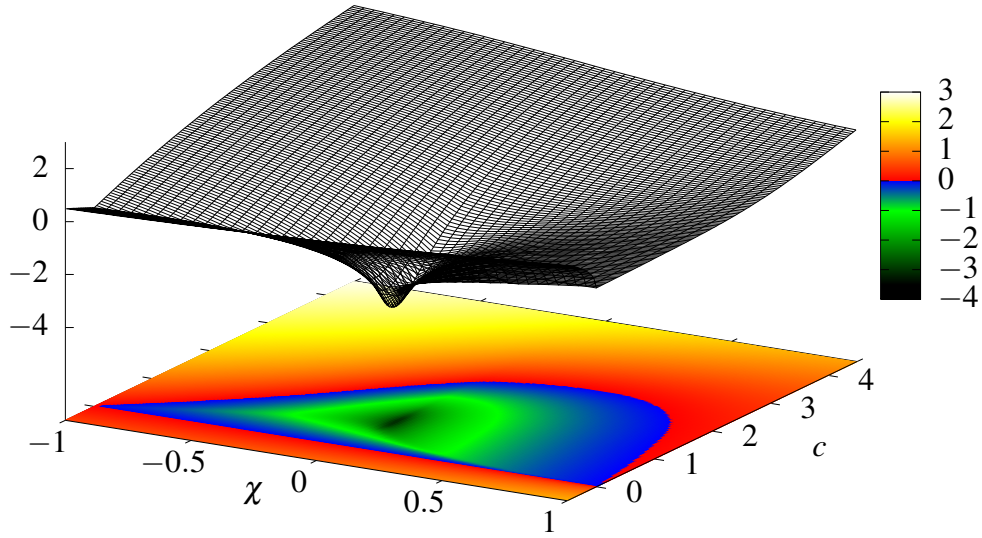


Figure 2: Expected value of $\Phi_{t+1} - \Phi_t$ if t tends to infinity.

As we can also use an approximation on $f_{\Delta,\infty}$ instead of $f_{\Delta,t}$ we can also evaluate the limit of expected difference of consecutive convergence indicators $\lim_{t \rightarrow \infty} \mathbb{E}[\Phi_{t+1} - \Phi_t]$.

3.3 Notes on the numerical evaluations

In Figure 2 one can see the expected difference of consecutive convergence indicators if t tends to infinity. We present data for parameter configurations $\chi \in [-1, 1]$ and $c_l = c_g = c \in [-0.5, 4.5]$. The sharp border between the blue and the red area delimits the parameter configurations where convergence can be expected. This delimitation is already displayed in Figure 1. In Table 1 for an established set of parameters also the expected difference of consecutive convergence indicators is presented. Figure 3 also displays the corresponding stationary distribution on the angles in comparison to an empirical probability density function, which is obtained by experiments. Also the value of the inner integral $f^{in}(\alpha) = \int_{l_H}^{u_H} g(\alpha, h) \cdot f_H(h) dh$ is visualized.

To evaluate this values we used spline interpolation with initially 64 equidistant knot points and increased the number of knot points adaptively to 2048 knot points for both types of splines used to calculate the next probability density function on the angles (see Section 3.1). Additional knot points are placed where the third derivative of calculated splines changes the most. We use periodic boundary conditions for the splines representing $F_{\Delta,t}$ in the sense that $F'_{\Delta,t}(-\pi/2) = F'_{\Delta,t}(\pi/2)$, $F''_{\Delta,t}(-\pi/2) = F''_{\Delta,t}(\pi/2)$ and obviously $F'_{\Delta,t}(-\pi/2) = 0 \neq 1 = F'_{\Delta,t}(\pi/2)$. For the spline approximating $\Pr[f^+(\tan(\alpha_t), h) \leq \tan(\beta_i)] \cdot f_H(h)$ for any value β_i we split this function into several pieces according to the cases for the function f_H (see Equation (7)) as we do not have continuous derivatives at these positions. For each part we use natural boundary conditions, i. e., the second derivative at boundary points is zero. We stop doing iterations if the \mathcal{L}_2 -norm of

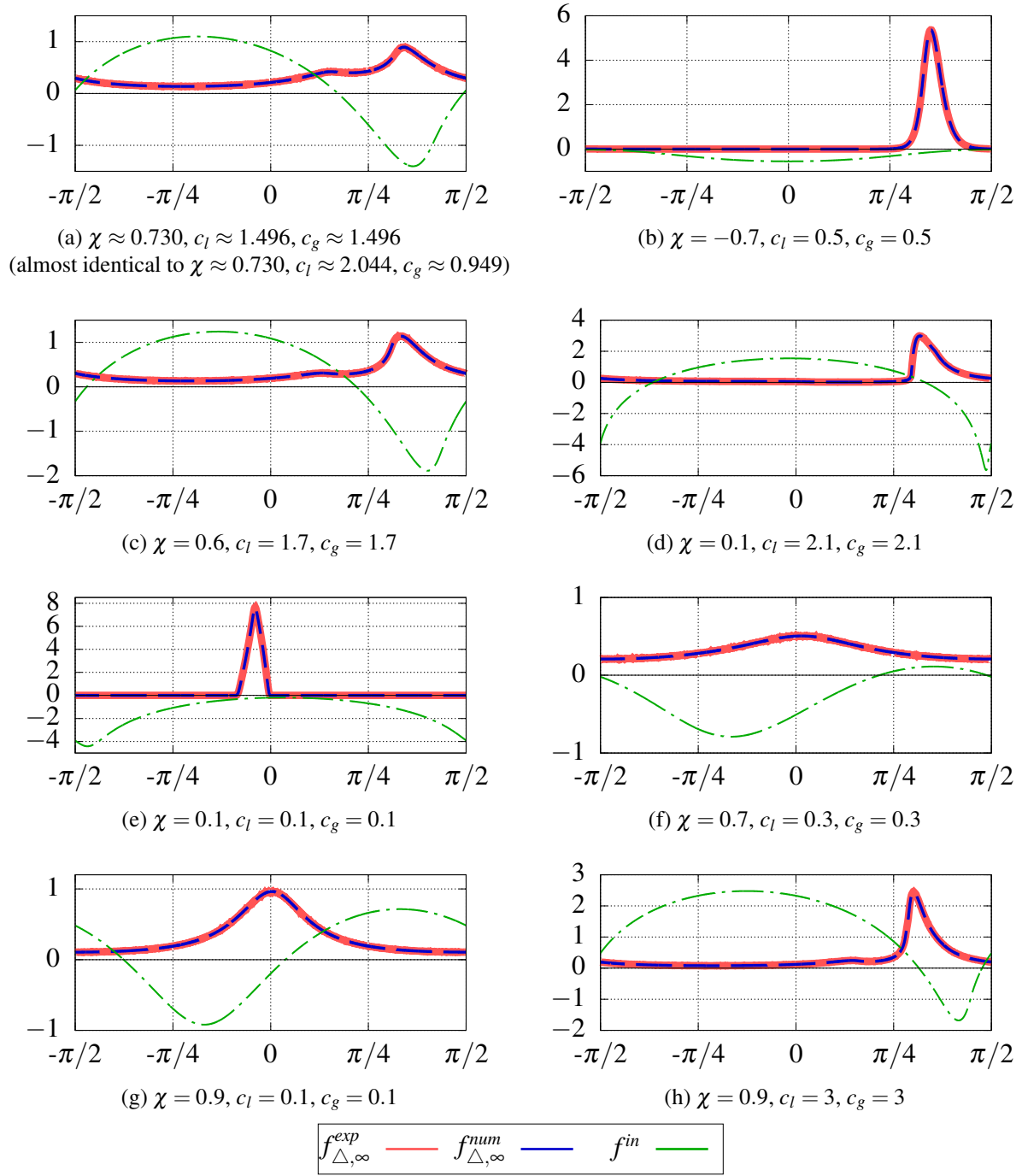


Figure 3: Comparison of experimental ($f_{\Delta, \infty}^{exp}$) and numerical ($f_{\Delta, \infty}^{num}$) probability density function. Additionally the respective inner integral $f^{in}(\alpha) = \int_{l_H}^{u_H} g(\alpha, h) \cdot f_H(h) dh$

Reference	χ	c_l	c_g	$\lim_{t \rightarrow \infty} \mathbb{E}[\Phi_{t+1} - \Phi_t]$
[CK02, ES00, Tre03]	0.72984	1.496172	1.496172	-0.194063
[CD01]	0.72984	2.04355	0.94879	-0.177108
[Tre03]	0.6	1.7	1.7	-0.327742
[Tre03]	0.9	0.1	0.1	-0.100728
[Tre03]	0.7	0.3	0.3	-0.338770
[Tre03]	0.9	3	3	0.380623
[Tre03]	0.1	0.1	0.1	-0.241938
[Tre03]	0.1	2.1	2.1	-0.485162
[Tre03]	-0.7	0.5	0.5	-0.133533

Table 1: Standard parameter sets and corresponding expected change in the logarithm of position and velocity

$F_{\Delta,t} - F_{\Delta,t+1}$ is at most 10^{-7} . Please note the \mathcal{L}_2 -norm of a function f is $\sqrt{\int_{\Omega} \|f(x)\|^2 d\mu(x)}$. Here the respective space Ω is $[-\pi/2, \pi/2]$ and for the measure μ we use the uniform distribution and consequently obtain $\sqrt{\int_{-\pi/2}^{\pi/2} (F_{\Delta,t}(\alpha) - F_{\Delta,t+1}(\alpha))^2 \cdot (1/\pi) \cdot d\alpha}$ for the \mathcal{L}_2 -norm. Usually this procedure reaches this tolerance after few ($\approx 100 - 400$) iterations, but especially in cases where $|\chi|$ is much larger than $|c_l|$ and $|c_g|$ many iterations are required (for $\chi = 1, c_l = c_g = 0.01$ we need ≈ 10000 iterations). To overcome periodic developments fast we keep a small portion of the old distribution for the next distribution.

For evaluation of Equation (24) we finally used 8192 knot points for both types of splines appearing in this task (see Section 3.2). Here natural boundary conditions are used for both types of splines, i. e., second derivative at boundary points is zero. The only problematic case here is $\chi = 0$ as then the inner integral f^{in} is $-\infty$ at the borders. In all other cases $f_{in}(\alpha) = \ln(2 \cdot \chi^2)$ if α is equal to $-\pi/2$ or $\pi/2$.

Nevertheless for all evaluations the absolute errors are less than 10^{-4} on the final result - this is even true for cases with $\chi = 0$, which could be reached by clipping the boundary by 10^{-15} . In most cases the error is considerably smaller ($\approx 10^{-7}$).

3.4 Comparison to Empirical Results

To supply further evidence that the obtained results are correct and no conceptual errors are present we compare the results with observations on experiments.

For experiments we analyzed a **single** PSO execution in a single dimension with a huge number of iterations (50000000) and evaluated the average difference of consecutive convergence indicators. There are several reasons for using only a single PSO execution instead of using multiple PSO executions. If we use multiple executions we can take into account only the iterations after the distribution of the current angle of the vector consisting of the position x and the velocity v is similar to the stationary limit distribution. Therefore we need to know how many iterations we have to make until the result is useful but this number of iterations can not be determined easily. Additionally for each PSO execution this first part of iterations costs much computing

power without benefit. Using the average of all differences of consecutive convergence indicators has the benefit that the share of the starting period becomes more and more negligible the longer the experiment is running. The covariance between differences of different iterations becomes smaller the further apart the iterations are. Therefore the average difference of consecutive convergence indicators measured on this single PSO execution converges to a normal distribution (also called Gaussian distribution). By estimating the variance of single differences of consecutive convergence indicators and the covariances of those also the variance of the average value can be estimated. While comparing the difference of the measured values and the numerically calculated values inversely scaled by the square root of the estimated variance among all evaluated test sets we observe characteristics of a normal distribution as expected, i. e., the relative frequency of large deviations conforms to quantiles of the normal distribution. Statistical tests on the equivalence do not make sense as the numerically calculated values are not exact. Especially for numerical results with larger errors (up to 10^{-4}) the estimated standard deviations are of the same magnitude as the numerical errors. Nevertheless, the experiments confirm the correctness of the numerical evaluations. As a reference we refer to Figure 3, where the numerically obtained limit distribution on the angles is compared with the experimentally obtained relative frequencies. The relative frequencies are evaluated for 1 000 blocks of equal size. The i th block captures the relative frequency of the interval $[-\pi/2 + (i - 1) \cdot \pi/1000, -\pi/2 + i \cdot \pi/1000)$. If n_i is the number of iterations such that the respective angle is in the i th block then the relative frequency is the number of iterations with an angle in that block divided by the number of all iterations and divided by the block length: $n_i \cdot 1000 / (\pi \cdot 50000000)$. Figure 3 shows that for all visualized parameter sets the numerically evaluated limit distribution coincides with the experimentally evaluated relative frequencies up to some noise in the relative frequencies.

4 Conclusion

Parameter selection for meta-heuristics is a topic that is widely regarded in the literature. In this paper we focus on the parameter selection for PSO and its influence on the convergence of the particle swarm. We introduce a new convergence indicator Φ_t that can be used to prove for a selection of parameters whether the swarm will finally converge or diverge. If in expectation the difference of two consecutive convergence indicators is negative the swarm will finally converge. We introduce a series of equations for calculating this difference of convergence indicators and explain how to numerically solve these equations using cubic spline interpolation where the results have only minor errors. Finally we provide experiments that confirm the correctness of presented equations and their numerical evaluation.

References

- [Bot03] Michael W. Botsko. An elementary proof of Lebesgue’s differentiation theorem. *The American Mathematical Monthly*, 110(9):834–838, 2003. doi:10.2307/3647803.

- [Can84] G. Cantor. De la puissance des ensembles parfaits de points: Extrait d'une lettre adressée à l'éditeur. *Acta Math.*, 4:381–392, 1884. doi:10.1007/BF02418423.
- [CD01] Anthony Carlisle and Gerry Dozier. An off-the-shelf PSO. In *Proceedings of the Workshop on Particle Swarm Optimization*, 01 2001.
- [CE15] C. W. Cleghorn and A. Engelbrecht. Fully informed particle swarm optimizer: Convergence analysis. In *2015 IEEE Congress on Evolutionary Computation (CEC)*, pages 164–170, May 2015. doi:10.1109/CEC.2015.7256888.
- [CK02] Maurice Clerc and James Kennedy. The particle swarm – explosion, stability, and convergence in a multidimensional complex space. *IEEE Transactions on Evolutionary Computation*, 6:58–73, 2002. doi:10.1109/4235.985692.
- [Dur10] R. Durrett. *Probability: Theory and Examples*. Cambridge Series in Statistical and Probabilistic Mathematics. Cambridge University Press, 2010. doi:10.1017/9781108591034.
- [ES00] R. C. Eberhart and Y. Shi. Comparing inertia weights and constriction factors in particle swarm optimization. In *Proc. Congress on Evolutionary Computation (CEC)*, volume 1, pages 84–88, July 2000. doi:10.1109/CEC.2000.870279.
- [Gaz12] V. Gazi. Stochastic stability analysis of the particle dynamics in the PSO algorithm. In *IEEE International Symposium on Intelligent Control (ISIC)*, pages 708–713, Oct 2012. doi:10.1109/ISIC.2012.6398264.
- [HEOB18] Kyle Robert Harrison, Andries P. Engelbrecht, and Beatrice M. Ombuki-Berman. Optimal parameter regions and the time-dependence of control parameter values for the particle swarm optimization algorithm. *Swarm and Evolutionary Computation*, 41:20–35, 2018. doi:10.1016/j.swevo.2018.01.006.
- [HM76] Charles A. Hall and W. Weston Meyer. Optimal error bounds for cubic spline interpolation. *Journal of Approximation Theory*, 16(2):105–122, 1976. doi:10.1016/0021-9045(76)90040-X.
- [JLY07a] M. Jiang, Y. P. Luo, and S. Y. Yang. Particle swarm optimization – stochastic trajectory analysis and parameter selection. In Felix T. S. Chan and Manoj Kumar Tiwari, editors, *Swarm Intelligence – Focus on Ant and Particle Swarm Optimization*, pages 179–198. 2007.
- [JLY07b] M. Jiang, Y. P. Luo, and S. Y. Yang. Stochastic convergence analysis and parameter selection of the standard particle swarm optimization algorithm. *Information Processing Letters*, 102:8–16, 2007. doi:10.1016/j.ipl.2006.10.005.
- [KE95] James Kennedy and Russell C. Eberhart. Particle swarm optimization. In *Proc. IEEE International Conference on Neural Networks*, volume 4, pages 1942–1948, 1995. doi:10.1109/ICNN.1995.488968.

- [OM99] E. Ozcan and C. K. Mohan. Particle swarm optimization: surfing the waves. In *Proc. Congress on Evolutionary Computation (CEC)*, volume 3, pages 1939–1944, July 1999. doi:10.1109/CEC.1999.785510.
- [Pol09] Riccardo Poli. Mean and variance of the sampling distribution of particle swarm optimizers during stagnation. *IEEE Transactions on Evolutionary Computation*, 13(4):712–721, 2009. doi:10.1109/TEVC.2008.2011744.
- [SW15] Manuel Schmitt and Rolf Wanka. Particle swarm optimization almost surely finds local optima. *Theoretical Computer Science*, 561, Part A:57–72, 2015. doi:10.1016/j.tcs.2014.05.017.
- [Tre03] Ioan Cristian Trelea. The particle swarm optimization algorithm: Convergence analysis and parameter selection. *Information Processing Letters*, 85:317–325, 2003. doi:10.1016/S0020-0190(02)00447-7.
- [vdBE02] F. van den Bergh and A. P. Engelbrecht. A new locally convergent particle swarm optimiser. In *Proc. IEEE Int. Conf. on Systems, Man and Cybernetics (SMC)*, volume 3, pages 94–99, 2002. doi:10.1109/ICSMC.2002.1176018.